Microbial footprints of tomato domestication

Sarango Flores, S.W.

Chapter 4

Microbiome-mediated tolerance of wild tomato to the invasive insect *Prodiplosis longifila*

Stalin Sarango Flores[1,2], Viviane Cordovez[1], Ben O. Oyserman[1], Luisa M. Arias Giraldo[1], Nejc Stopnisek[3], Jos M. Raaijmakers[1,2], Pieter van 't Hof[4,5]

[1] Department of Microbial Ecology, Netherlands Institute of Ecology, Wageningen, 6708PB, Netherlands
[2] Institute of Biology, Leiden University, Leiden, 2333BE, Netherlands
[3] Department of Microbiological Research, National Laboratory of Health, Environment and Food, Maribor, 2000, Slovenia
[4] Colegio de Ciencias Biológicas y Ambientales, Universidad San Francisco de Quito USFQ, Quito, 170901, Ecuador
[5] Instituto de Microbiología, Colegio de Ciencias Biológicas y Ambientales, Universidad San Francisco de Quito USFQ, Quito, 170901, Ecuador

A modified version has been published in *Environmental Microbiology Reports 2025, 17*(5), e70190
doi: https://doi.org/10.1111/1758-2229.70190

Abstract

Plant roots are colonized by diverse communities of microorganisms that can affect plant growth and enhance plant tolerance to (a)biotic stresses. Here, we investigated the role of the indigenous soil microbiome in tolerance of tomato to the invasive sap-sucking insect *Prodiplosis longifila* (Diptera: Cecidomyiidae). Native and agricultural soils were sampled from the Andean region in Southern Ecuador and tested, in greenhouse bioassays, for leaf tissue damage caused by *P. longifila* on domesticated *Solanum lycopersicum* cv. Moneymaker and wild tomato *S. pimpinellifolium*. We observed no significant differences in insect damage between domesticated and wild tomatoes grown in live native or agricultural soils. However, when grown in sterilized native and agricultural soils, wild tomato was more severely affected by the insect than the domesticated tomato. Subsequent microbiome analyses revealed that soil sterilization impacted overall rhizobacterial diversity and abundance in the wild tomato. Particularly, the abundance of *Actinoplanes* was reduced upon sterilization which significantly correlated with loss of insect tolerance. Metagenome analyses and subsequent genome assembly of Micromonosporaceae (*Actinoplanes* family) suggested a putative association between motility, chemotaxis, membrane transport, chorismate and lanthipeptide biosynthesis and insect tolerance. Collectively, these results indicate that wild tomato *S. pimpinellifolium,* in contrast to domesticated *S. lycopersicum,* relies on specific members of the root-associated microbiome for protection against the endemic insect *P. longifila*.

Keywords: center of origin, indigenous microbiome, *Prodiplosis* tolerance, rhizosphere *Actinoplanes*, tomato

Introduction

Root-associated microorganisms contribute to plant growth and health via the production of hormones, enhanced nutrient acquisition and protection from pathogens and insect pests (Carrillo et al., 2019; Choi et al., 2020; Lee et al., 2021; Meshram & Adhikari, 2024; Pineda et al., 2017; Smulders et al., 2021; Tronson et al., 2022). Most of the current knowledge on how soil- and root-associated microorganisms impact aboveground insect herbivory arises from single microorganisms and modern crop cultivars grown under controlled conditions in greenhouse soils (Friman et al., 2021; Rashid & Chung, 2017; van de Mortel et al., 2012). However, research on how root-associated microbiomes of wild crop relatives in native habitats impacts plant fitness, including tolerance to insects, remains largely unknown. In this context, it has been postulated that wild crop relatives and their native microbiomes have co-evolved to withstand (a)biotic stresses (Barajas et al., 2020; Pérez-Jaramillo et al., 2016; Wallenstein, 2017). In contrast, environmental disturbances within agricultural systems combined with genetic modifications by plant breeding may have led to the loss of beneficial interactions between domesticated plants and their microbiome (Cordovez et al., 2019; O'Brien et al., 2021; Oyserman et al., 2021). To begin to understand the role of the soil and root microbiome in protection of wild crop relatives against (a)biotic stresses, we sampled native and agricultural soils from the Andean region in Southern Ecuador and tested these soils in greenhouse bioassays with domesticated *Solanum lycopersicum* and wild tomato *S. pimpinellifolium* for leaf tissue damage caused by the insect *Prodiplosis longifila* Gagné (Diptera: Cecidomyiidae) (Figure 1). This sap-sucking invasive insect is an economically important pest of tomato and other solanaceous crops in South America (Duque-Gamboa et al., 2018; Hernandez et al., 2015; Valarezo Cely et al., 2003; Velasco-Cuervo et al., 2016) and designated a priority for Pest Risk Analysis (PRA) by the EPPO Panel on Phytosanitary measures (EPPO, 2017). It can cause up to 100% loss of tomato in Colombia and up to 60% loss in Ecuador (Constante Tubay et al., 2023; Valarezo Cely et al., 2003).

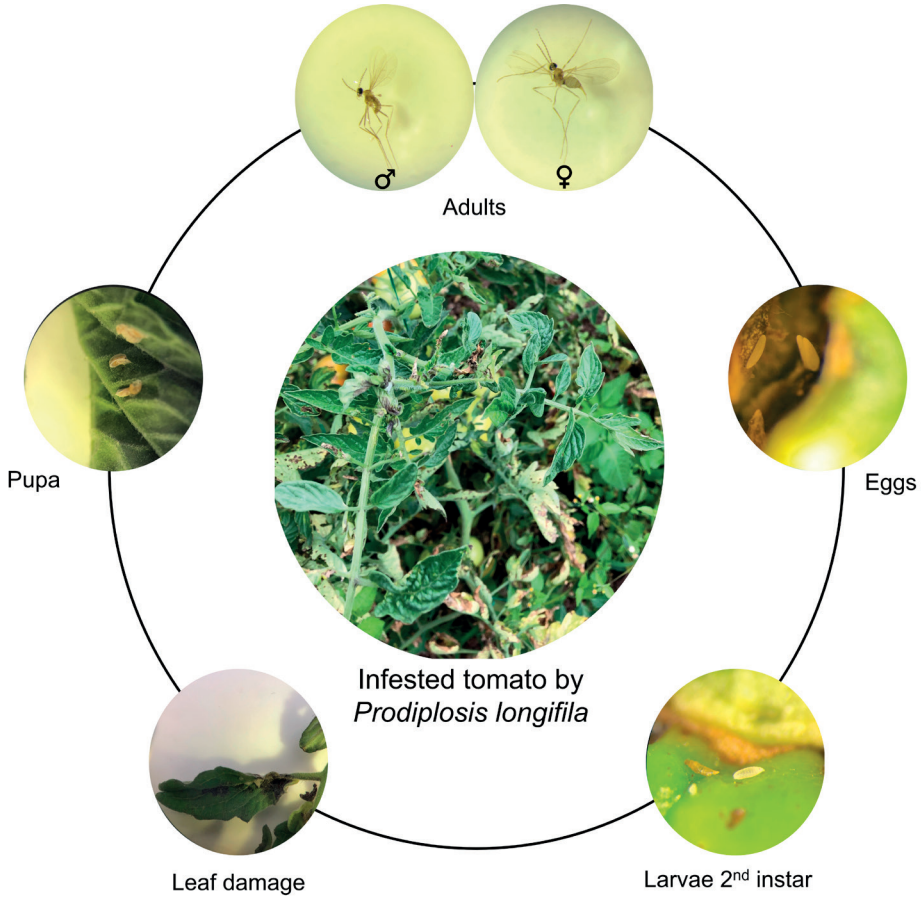

Figure 1. *Prodiplosis longifila* (Diptera: Cecidomyiidae) life cycle (Pictures by SSF). In the center panel, severe damage of tomato (*S. lycopersicum* cv. Elpida) field crop grown in Loja, Ecuador. In the outer panel, a summary of the life cycle. Larve 2nd instar were used to infest greenhouse grown tomato and leaf damage was assessed 7 days after infestation (bottom two panels).

Chapters 2 and 3 demonstrated how the tomato root microbiome is assembled by native habitats, domestication and agricultural management, revealing both conserved microbial signatures and functional shifts across soils and genotypes. Building on these results, Chapter 4 investigates the ecological consequences of microbiome variation by focusing on plant–insect interactions. Specifically, we assessed the role of the native rhizosphere microbiome in protecting tomato against the sap-feeding insect *Prodiplosis longifila*.

To evaluate the protective potential of the tomato microbiome against this insect pest, we 1) assessed the role of the microbiome of native and agricultural soils on tomato leaf damage by *P. longifila;* 2) performed a comparative analyses of the rhizosphere

microbiome composition of wild tomato *S. pimpinellifolium* and domesticated tomato *S. lycopersicum*; and, 3) conducted metagenomics on soils with contrasting phenotypes to identify putative microbial traits associated with protection of wild tomato against *P. longifila.* We found that microbiome disruption by soil sterilization caused a significant increase of leaf damage by *P. longifila* in wild tomato grown in native and agricultural soils, but not in domesticated tomato. The taxonomic diversity of the tomato rhizosphere bacterial microbiome was different between native and agricultural soil, but no substantial differences in taxonomic composition were observed between domesticated and wild tomato. Interestingly, we found a significant negative correlation between the relative abundance of several rhizobacterial taxa, in particular *Actinoplanes,* and insect leaf damage in wild tomato. Subsequent metagenome analyses pinpointed putative traits of *Actinoplanes,* including motility, chemotaxis, membrane transport, and secondary metabolism, that significantly correlated with insect tolerance.

Results

Impact of tomato genotype and soil condition on insect leaf damage

Insect larvae caused significant leaf damage among the treatments (ANOVA, Soil * Condition, p = 0.04043). Both the domesticated tomato *S. lycopersicum* cv. Moneymaker and wild tomato *S. pimpinellifolium* showed low levels of insect leaf damage when grown in agricultural (4.70% and 4.39%, respectively) or native soils (3.48% and 6.98%, respectively) (Figure 2). When the agricultural and native soils were sterilized, the domesticated tomato cultivar remained tolerant to insect leaf damage. In contrast, significantly more insect leaf damage was observed when the wild tomato was grown in sterilized agricultural and native soils, compared with the respective live soils (Figure 2). Insect leaf damage on wild tomato increased to an average of 16.5% and 15.0% in agricultural and native soils, respectively. In contrast, no significant change was observed for insect leaf damage on the modern tomato cultivar grown in sterilized agricultural and native soils. These results indicate that the wild tomato, in contrast to the domesticated tomato, relies on the soil (micro)biome for protection against *P. longifila*.

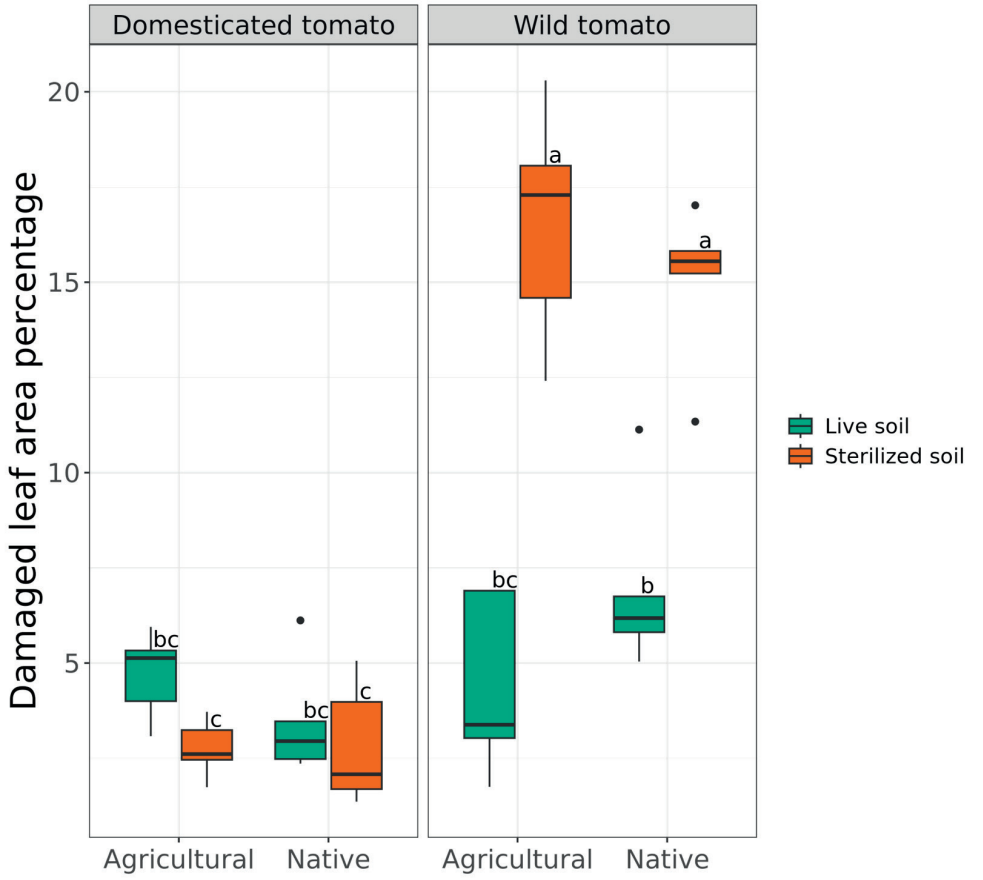

Figure 2. Leaf damage by *Prodiplosis longifila* on domesticated tomato *S. lycopersicum* cv. Moneymaker and wild tomato *S. pimpinellifolium* grown for 41 days in live and sterilized native and agricultural soils. Bars represent the standard deviations of the mean of five replicates. Significant differences in percentage of insect leaf damage between the domesticated and wild tomato plants grown in two soils are indicated by different letters (Tukey HSD post hoc test $p < 0.05$).

Effect of soil sterilization on tomato rhizosphere microbiome composition

Alpha diversity of rhizosphere bacterial communities was significantly higher for tomato plants grown in the live soil as compared to plants grown in the sterilized soils (ANOVA, p = 9.9e-13). This was reflected in higher Shannon indices for tomato plants grown in live soils as compared to sterilized soils (Figure 3a). Significant differences in beta diversity were found between agricultural and native soils (PERMANOVA, p = 0.0035), however, no differences were found between the wild and domesticated tomato in overall composition of the rhizobacterial community (Figure 3b).

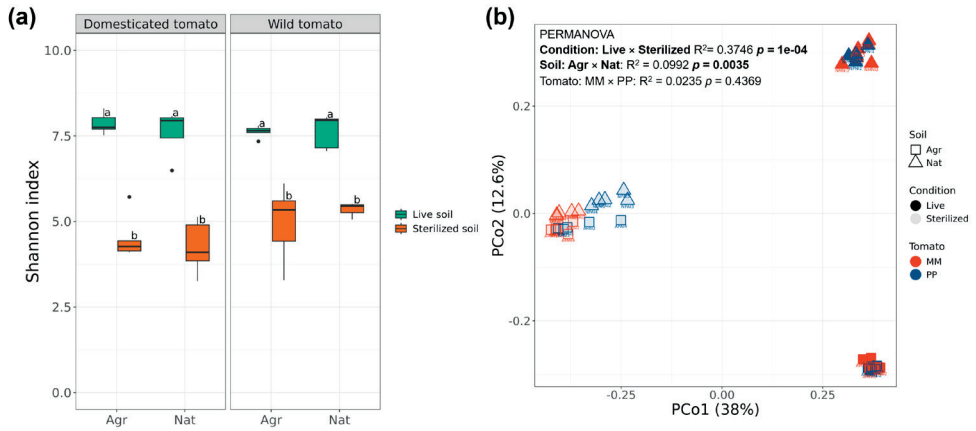

Figure 3. (a) Shannon diversity index of bacterial communities in the rhizosphere of domesticated *S. lycopersicum* cv. Moneymaker and of wild tomato *S. pimpinellifolium* grown in live and sterilized native and agricultural soils. Boxplots represent the mean of five replicates. Significant differences between soils and tomato genotypes are indicated by different letters (Tukey HSD post hoc test $p < 0.05$); **(b)** PCoA of bacterial rhizosphere of domesticated *S. lycopersicum* cv. Moneymaker (MM) and wild *S. pimpinellifolium* (PP) tomato infested by *Prodiplosis longifila* in different soil type (Agr: agricultural; Nat: native) and soil condition (Live; Sterilized).

Changes in wild tomato rhizosphere composition by soil sterilization correlate with leaf damage

To identify correlations between changes in the rhizobacterial community composition and the level of leaf damage caused by *P. longifila*, amplicon data of the wild tomato grown in live or sterilized native and agricultural soils were subjected to differential abundance analysis. This analysis showed that 404 ASVs were shared between live agricultural and native soils, whereas 209 ASVs were shared between sterilized agricultural and native soils (Supplementary Figure S2). We observed an impact of soil sterilization on the relative abundance of specific members of the phyla Actinobacteriota, Acidobacteriota, Chloroflexi, Cyanobacteria, Gemmatimonadota and Myxococcota (Figure 4a). More specifically, the genera *Actinoplanes, Sphingomonas, RB41, Geodermatophilus* and *MND1* had a higher relative abundance in live soils (i.e. lower in sterilized soils), while the abundance of *Nocardioides, Methylobacterium, Pseudomonas, Paenarthrobacter* and *Pseudoarthrobacter* was higher in sterilized soils (Figure 4b).

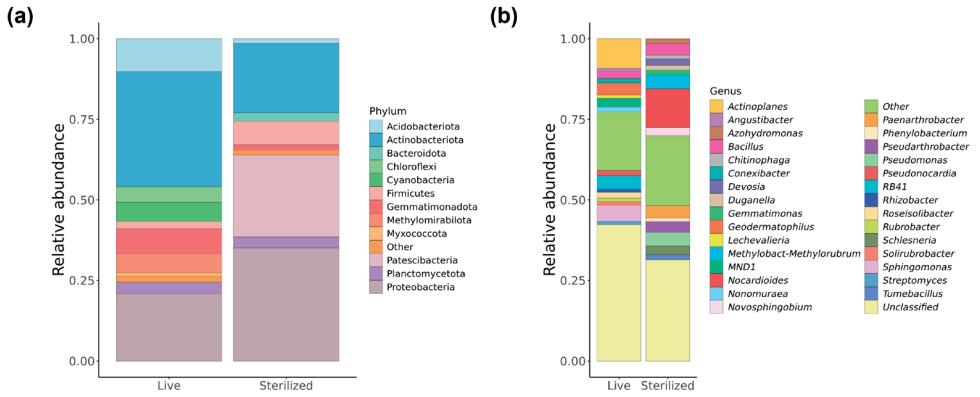

Figure 4. Composition of bacterial phyla **(a)** and genera **(b)** in the rhizosphere of wild tomato *S. pimpinellifolium* in live and sterilized soil conditions; significant differential ASVs shared among live and sterilized agricultural and native soils were grouped according to their phylum or genus and plotted as stacked bar charts; "Other" category corresponds to grouped phyla or genera with relative abundance < 0.01.

To investigate the relationships between insect leaf damage and the abundance of specific rhizobacterial taxa, we performed Spearman correlation analysis and a more stringent analysis based on linear regression modelling. Spearman correlation analysis showed a significant correlation between rhizobacterial abundance and insect leaf damage (ρ Spearman ≥ 0.64; Supplementary Figure S3). Further analysis using linear regression modelling predicted significant negative correlations between insect leaf damage and the relative abundance of *Actinoplanes* (R^2 = 0.7677), *MND1* (R^2 =0.6786), *RB41* (R^2 = 0.6748), and *Geodermatophilus* (R^2 = 0.6668). Positive correlations were predicted for *Nocardioides* (R^2 = 0.6982), *Paenarthrobacter* (R^2 = 0.499), *Methylobacterium* (R^2 = 0.462), and *Pseudomonas* (R^2 = 0.6278) (Figure 5). No significant correlations were found between *Sphingomonas* (Figure 5e) and *Pseudoarthrobacter* (Figure 5i) abundances and the proportion of insect leaf damage. Collectively these correlations suggest that a higher relative abundance of *Actinoplanes* and some other genera was associated with lower levels of insect damage, while a higher relative abundance of *Nocardioides* and some other bacterial genera was associated with higher levels of insect damage (Figure 4 and 5).

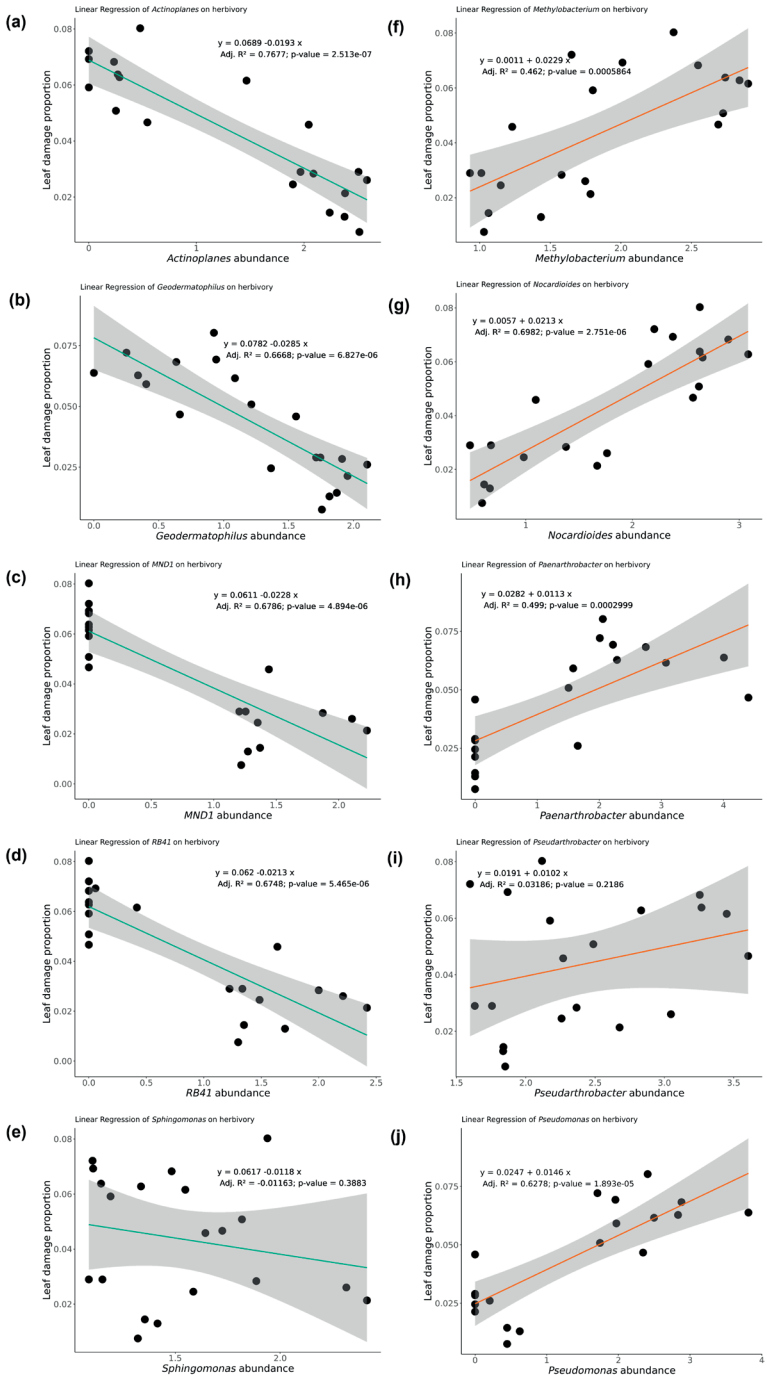

Figure 5. Linear regression models describing the relationship between the abundance of **(a)** *Actinoplanes*, **(b)** *Geodermatophilus*, **(c)** *MND1*, **(d)** *RB41*, **(e)** *Sphingomonas*, **(f)** *Methylobacterium*, **(g)** *Nocardioides*, **(h)** *Paenarthrobacter*, **(i)** *Pseudarthrobacter*, and **(j)** *Pseudomonas* and leaf damage. Leaf damage percentage and absolute abundance data (n = 10) were log10(x+1) transformed.

Functional features of key rhizobacterial genera associated with leaf damage

To get preliminary insight into the functional traits of the two bacterial genera *Actinoplanes* and *Nocardioides*, taxa that negatively or positively correlated to insect damage, respectively, we performed shotgun sequencing with a pooled set of rhizosphere soil samples (five replicates of each treatment, each consisting of eight pooled samples). Two MAGs (high quality bins completeness >70%, contamination <10%) were classified as Micromonosporaceae (*Actinoplanes* family) (bin 580, completeness 88.42%, contamination 2.59%) and *Nocardioides* (bin 2.78, completeness 72.60%, contamination 5.66%) (Supplementary Table S1). To investigate their functional traits, the MAGs were annotated using RAST (Supplementary Table S2) and antiSMASH. '*Actinoplanes* bin 580' showed higher number of protein-encoding genes (883) than '*Nocardioides* bin 2.78' (715). '*Actinoplanes* bin 580' was characterized by motility & chemotaxis and secondary metabolism SEED categories, which were absent in '*Nocardioides* bin 2.78'. Moreover, '*Actinoplanes* bin 580' showed higher number of genes involved in membrane transport; nitrogen metabolism; protein metabolism; secondary metabolism; sulfur metabolism; and virulence, disease and defense SEED categories. In contrast, '*Nocardioides* bin 2.78' showed more genes related with amino acids and derivatives; carbohydrates; cofactors, vitamins, prosthetic groups, pigments; fatty acids, lipids and isoprenoids; metabolism of aromatic compounds; phosphorus metabolism; and stress response SEED categories (Figure 6).

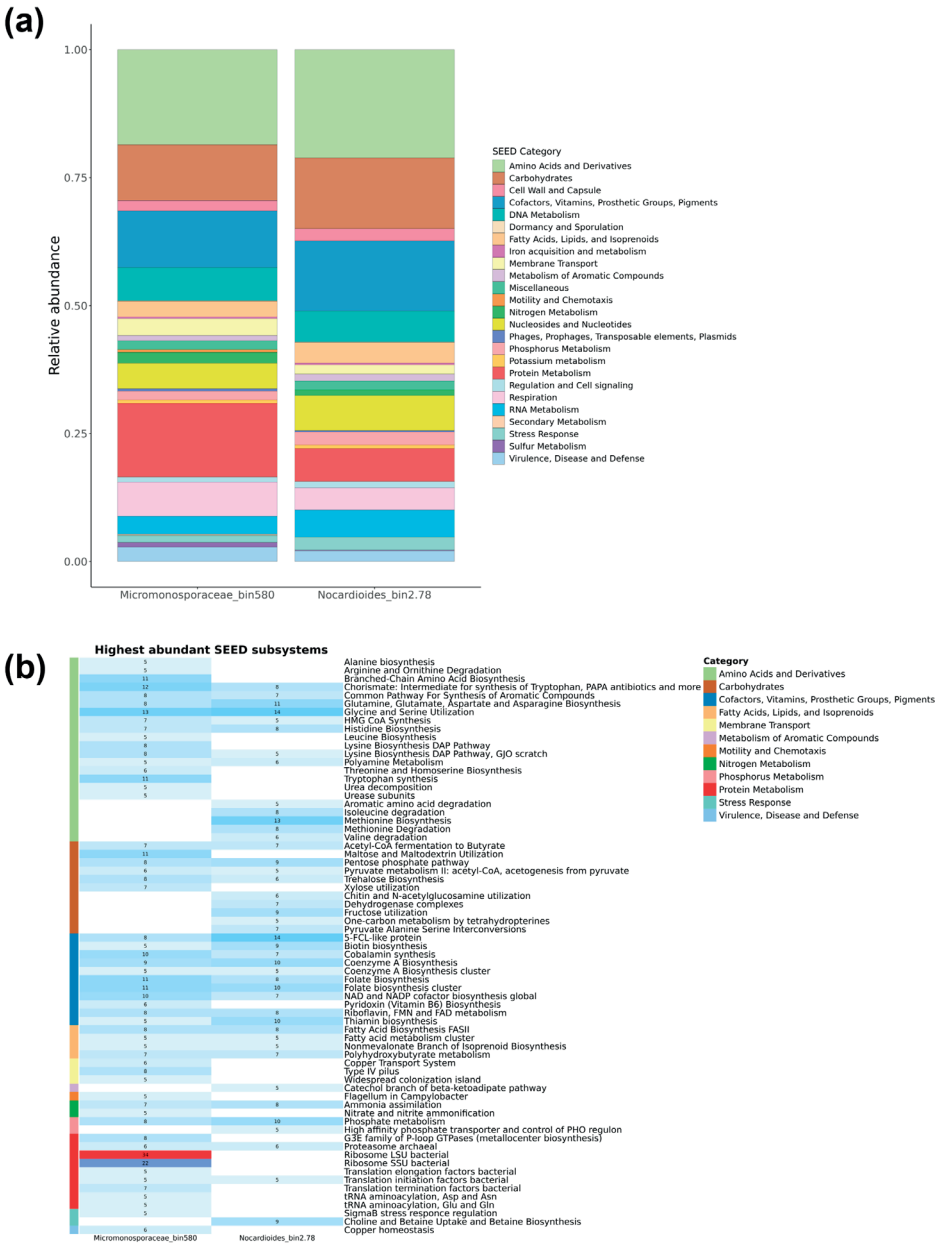

Figure 6. (a) Relative abundance of SEED Categories annotated by RAST (Rapid Annotation using Subsystems Technology) of two bacterial genera *Actinoplanes* and *Nocardioides* from the rhizosphere of wild tomato *S. pimpinellifolium* that showed a negative and positive correlation, respectively, with *Prodiplosis longifila* leaf damage; the relative abundance of protein encoding genes were grouped in their respective SEED Categories and plotted as stacked bar charts; **(b)** Heatmap of main SEED Subsystems showing the number of protein encoding genes.

A total of 11 BGCs were identified for *Actinoplanes* bin 580 and 1 BGC for *Nocardioides* bin 2.78. From these, 3 BGCs of '*Actinoplanes* bin 580' were annotated as a type III polyketide synthase biosynthetic gene cluster predicted to encode loseolamycins A1 and A2, aminopolycarboxylic-acid biosynthetic gene cluster of the siderophore ethylenediaminesuccinic acid hydroxyarginine (EDHA) and the terpene isorenieratene, albeit with low similarity. For '*Nocardioides* bin 2.78', no specific BGCs could be annotated by antiSMASH (Table 1; Supplementary Figure S4 and S5).

Table 1. Biosynthetic gene clusters (BGCs) predicted by antiSMASH bioinformatics tool from bins of Micromonosporaceae bins 580 and *Nocardioides* bin 2.78 enriched in the rhizosphere of the wild tomato *S. pimpinellifolium* infested by *Prodiplosis longifila* in live and sterilized soil, respectively.

Bin ID	Length (nt)	BGC type	Secondary metabolite	Similarity	Reference in MiBIG database	Organism in MiBIG database
Actinoplanes bin 580	23,195	T3PKS	Loseolamycin A1, Loseolamycin A2	64%	BGC0002362	*Micromonospora endolithica*
Actinoplanes bin 580	13,418	Aminopolycarboxylic-acid	EDHA	88%	BGC0002568	*Streptomyces scabiei* 87.22
Actinoplanes bin 580	10,650	Terpene	Isorenieratene	25%	BGC0000664	*Streptomyces griseus* subsp. *griseus* NBRC 13350
Nocardioides bin 2.78	2,627	RRE-containing	NA	NA	NA	NA

Discussion

It has been postulated that wild crop relatives and their native microbiomes have co-evolved to withstand (a)biotic stresses (Barajas et al., 2020; Pérez-Jaramillo et al., 2016; Wallenstein, 2017). In contrast, environmental disturbances within agricultural systems combined with genetic modifications by plant breeding may have led to the loss of beneficial interactions between domesticated plants and their microbiota (Cordovez et al., 2019; O'Brien et al., 2021; Oyserman et al., 2021). In our study, we observed no significant differences in leaf damage by the sap-sucking invasive insect *P. longifila* on both domesticated and wild tomatoes grown in live native or agricultural soils. However, microbiome disruption by soil sterilization caused a significant increase of insect leaf damage in wild tomato grown in native and agricultural soils, but not in domesticated tomato. These results suggest that wild tomato *S. pimpinellifolium,* in contrast to domesticated *S. lycopersicum,* relies on specific members of the root-associated microbiome for protection against the invasive insect *P. longifila* aboveground. It also suggests that the domesticated tomato has an intrinsic resistance to the invasive insect, that

operates largely independently from the soil microbiome. Previous study by Carrillo et al. (2019) found that tomato's resistance to herbivory by *Manduca sexta* (Lepidoptera: Sphingidae) was not dependent on tomato domestication or soil type. However, they observed that the wild tomato *S. pimpinellifolium,* grown consecutively in the same soil, i.e. 'tomato soil', attracted more parasitoid *Cotesia congregate* (Hymenoptera: Braconidae) compared to the domesticated tomato *S. lycopersicum*. In our experimental design under controlled greenhouse conditions, the attraction of parasitoids did not play a role. Most likely, insect tolerance in our experiments is due to root colonization and priming the plants' defense mechanisms (Pieterse et al., 2014) to resist insect attack.

Subsequent analyses showed that heat sterilization of the soils led to a significant increase in leaf damage of wild tomato when grown in both agricultural and native soils (Figure 2). Soil sterilization significantly reduced the alpha-diversity of the bacterial community in the rhizosphere of tomato grown in native and agricultural soils (Figure 3a). The differences observed in the rhizosphere microbiome composition were primarily due to the soil type (agricultural, native) and soil condition (live, sterilized), rather than the tomato genotype (Figure 3b; Supplementary Figure S1). This is consistent with previous studies indicating that soil exerts a stronger effect on rhizosphere assembly than plant host genotype (Cheng et al., 2020; French et al., 2020; Kandasamy et al., 2021; Smulders et al., 2021). Although rhizosphere microbiome assembly was similar for both tomato genotypes, the microbiome changes in the rhizosphere of wild tomato grown in sterilized soil suggested a putative role of the rhizosphere microbiome to minimize leaf damage by *P. longifila*. A comparable effect was found in *S. pimpinellifolium* infested by the aphid *Macrosiphum euphorbiae*, whose degree of infestation was influenced by the soil microbiome. Specifically, higher microbial diversity reduced aphid infestation (French et al., 2021). Moreover, negative impact on insect performance or less damage on plants grown in intact native microbiome has been previously described by Badri et al. (2013) for *Arabidopsis thaliana* and by Hubbard et al. (2019) for the crucifer *Boechera stricta*.

Differential abundance analyses further revealed that the abundance of several bacterial phyla was affected by soil sterilization, such as Actinobacteriota, Acidobacteriota, Chloroflexi, Cyanobacteria, Gemmatimonadota and Myxococcota (Figure 4a). Members of the phyla Actinobacteriota and Cyanobacteria have been investigated for the production of insecticidal compounds (Berry et al., 2008; Kaur et al., 2014; Nassar et al., 1999; Sharanappa et al., 2023; Silva et al., 2022). More specifically, *Streptomyces* spp. have been reported as a source of insecticides with potent larvicidal activity (Amelia-Yap et al., 2022, 2023; Balakrishnan et al., 2017). Here we found *Actinoplanes, Sphingomonas, RB41, Geodermatophilus* and *MND1* to be more abundant in the rhizosphere of wild tomato grown in live soil, while *Nocardioides, Methylobacterium,*

Pseudomonas, Paenarthrobacter and *Pseudoarthrobacter* were more abundant in the rhizosphere of tomato grown in sterilized soil (Figure 4b). With the exception of *Sphingomonas* and *Pseudoarthrobacter*, these bacterial genera showed a significant positive or negative correlation with the proportion of leaf damage caused by *P. longifila* (Figure 5). Interestingly, the abundance of *Actinoplanes* taxa was negatively correlated with leaf damage, whereas the abundance of *Nocardioides* taxa was positively correlated (Figure 5a and 5g). *Actinoplanes* spp. have been studied for their potential as insecticidal agents against other dipteran species such as *Drosophila melanogaster* (Diptera: Drosophilidae) (Al-Kaabi, 2004) and *Aedes aegyptii* (Diptera: Culicidae) (Balakrishnan et al., 2017; Hozzein, 2017). Nevertheless, these studies primarily focused on the activity of these microbial compounds applied directly onto the insects, rather than harnessing the ability of specific microorganisms to activate plant defense mechanisms (Choi et al., 2020; Lee et al., 2021; Ling et al., 2022; Pineda et al., 2017, 2020). Additional experiments, involving isolation of *Actinoplanes* and *Nocardioides* spp., insect bioassays and mechanistic analyses, will be needed to validate the putative roles of these two and possibly other rhizobacterial genera in protection of wild tomato against *P. longifila*. Extensive attempts to isolate *Actinoplanes* from wild tomato rhizosphere have not yet been successful.

Nevertheless, our analysis of the metagenome-assembled genome (MAG) *Actinoplanes* 580 did provide some first insights into the functional features that may be associated with wild tomato's tolerance to *P. longifila* (Figure 6b; Supplementary Table S2). Among these, motility & chemotaxis SEED subsystem was characterized by flagellar functions such as genes encoding synthesis of peptidoglycan (FtsI) and flagellin (FlaA, FlgB, FlgC and FliE). These genes are involved in activating bacterial division and assembling the protein components of the flagellum (Jang et al., 2016; Nedeljković et al., 2021; Tsang & Bernhardt, 2015). Flagella are required for bacterial motility and colonization and adherence to host surfaces (Guerry, 2007; Palleroni, 1976; Uchida et al., 2011). Flagella and pili are distinctive features of *Actinoplanes* zoospores (Kimura et al., 2019; Uchida et al., 2011). Particularly, pilus genes found in 'bin 580', such as PilB, PilC, PilM and PilT, may allow *Actinoplanes* zoospores to colonize and adhere to the tomato root surface (Kimura et al., 2019). Complementarily, within 'bin 580', genes of the widespread colonization island subsystem included tight adherence (TAD) genes, such as TadA, TadB, TadC and TadZ, and the pilin-encoding gene Flp, suggest *Actinoplanes*' capacity to colonize host tissues and surfaces of several environmental habitats (Planet et al., 2003). Furthermore, motility features have been described to be related with bacterial niche differentiation in high carbon availability as the rhizosphere (Ramoneda et al., 2024; Wu et al., 2023). Moreover, the presence of genes encoding lanthionine synthetases (LanB, LanL) of the secondary metabolism SEED category, suggest the potential for the biosynthesis of lanthipeptides, which have demonstrated antimicrobial

activity against Gram-positive bacteria by disrupting cell wall biosynthesis (Li et al., 2021; van Staden et al., 2021) as well as immunomodulatory activity (Ramírez-Rendón et al., 2023). Additionally, lanthipeptides can exert a regulatory role for aerial hyphae formation with limited antimicrobial activity in some actinobacteria (Holtsmark et al., 2008; Kodani et al., 2005). Furthermore, genes encoding amino acids and derivatives in 'bin 580' suggest the biosynthesis of chorismate, which is precursor of several secondary metabolites such as aromatic compounds, including tryptophan, involved in electron transport, signaling communication, plant defense and wound response (Corpas et al., 2021; Macheroux et al., 1999; Mishra & Baek, 2021). In particular, features of the biosynthesis of chorismate and aromatic amino acids may modulate plant defense response against *P. longifila,* which has been demonstrated in other studies on induced resistance against bacterial pathogens and phloem-feeding insects (Assis et al., 2021; Blundell et al., 2020; Shi et al., 2016). Last but not least, we also detected a putative cluster for the biosynthesis of the terpene isorenieratene, which is characteristic for certain Actinobacteria to cope with oxidative stress (Benaud et al., 2021; Krügel et al., 1999). The antiSMASH results also suggest that *Actinoplanes* harbors various underexploited natural products. These findings further emphasize the importance to isolate *Actinoplanes* spp., test their biosynthetic potential and determine the putative role of these metabolites in protection of wild tomato against *P. longifila.*

In conclusion, the results from this study highlight the potential of exploring center-of-origin soils that harbor viable populations of close relatives of economically important modern crops. Such soils may serve as valuable microbial reservoirs of tolerance to various pests and diseases. This is a promising area of research, particularly in understanding how belowground microbial communities, in conjunction with specific plant genotypes, can potentially promote tolerance to aboveground insect pests. Therefore, the integration of genomic approaches, involving the validation of key microbial taxa, along with the assessments of plant metabolites and defense hormones, will be essential to establish and validate the mechanistic links between microbial communities and plant defense pathways. Clarifying these dynamics and the modes of action of these 'ancestral microbiota' (Raaijmakers & Kiers, 2022) could pave the way for designing innovative agricultural practices that harness natural soil microbiomes to improve crop resilience.

Materials and Methods

Soil sampling and processing

Agricultural and native soils were collected in Zapotillo (Loja province, Ecuador). Agricultural soil was collected from a recently harvested corn farm close to the Cata-

mayo river (El Coco site, 4°22'44.0"S, 80°14'11.8"W), while native soil was collected from the right bank of the Alamor river (La Ceiba site, 4°18'07.6"S, 80°13'16.7"W) from a patch with natural vegetation mainly consisting of: *Prosopis juliflora* (Fabaceae), *Croton wagneri* (Euphorbiaceae), *Ipomoea purpurea* (Convolvulaceae), *Cromolaena* sp. (Asteraceae), *Parthenium hysterophorus* (Asteraceae), *Hyptis* sp. (Lamiaceae), and wild tomato *S. pimpinellifolium* (Solanaceae). Soils were transported to the greenhouse of the National University of Loja, air-dried for seven days at room temperature, sieved (2-mm-diameter mesh) to remove stones and plant debris, and stored at room temperature in the shade until further processing.

Experimental design

Domesticated tomato *Solanum lycopersicum* cv. Moneymaker and its close wild relative *S. pimpinellifolium* were grown in native and agricultural soils. In order to enrich the soil with rhizosphere microorganisms, live soils passed a 'microbial activation' phase which consisted of growing tomatoes in the agricultural and native soils for 30 days prior to the experiment. Afterwards, the complete plants and roots were removed from each pot, and half of the soil volume was subjected to heat sterilization (1.5 atm and 121 ºC, 1 h, for two consecutive times with 24 h in between) whereas the other half of the activated soil remained untreated. Tomato seeds were surface sterilized with 5 ml of ethanol 80% (v/v) and vortexed for 2 min. Then, the ethanol was removed and 5 ml of sodium hypochlorite 1.5% (v/v) was added, vortexed for 10 min and discarded. Finally, five washing cycles were done with 5-ml volumes of sterile demi water, vortexing for 2 min and removal of the water. The seeds were then placed on a wet filter paper in a Petri dish containing 5 ml of sterile demi water and incubated at 25 ºC for two days. Before sowing the seeds, each soil type was moistened by adding 10% (v/w) of water and distributed in pots (350 g per pot). In each pot, three pre-germinated seeds (radicle length ~1 cm) were sown at 2-cm depth and after the seedlings emerged, two were removed to obtain one single seedling per pot. This allowed us to have seedlings with uniform sizes across the different treatments. The experiment consisted of 2 tomato genotypes × 2 soil types (agricultural, native) × 2 soil conditions (live, sterilized) × 5 replicates, for a total of 40 experimental units, which were organized in a completely randomized design. Considering the differences in growth between domesticated and wild tomatoes, watering was done with tap water on a total pot weight basis. Plants were grown for 34 days under greenhouse conditions (temperature day/night: 25/22 ºC; relative humidity 60%; 12 h natural light) until the 4th true-leaf developmental stage.

Insect infestation

The insect *Prodiplosis longifilia* Gagné (Diptera: Cecidomyiidae) was used to infest tomato leaves. Infested leaves with *P. longifila* larvae were collected from a tomato field

(*S. lycopersicum* cv. Elpida) at fruiting stage in Catamayo (Loja, Ecuador, 3°54'51.4"S, 79°19'45.8"W) and transported in a cooler to the greenhouse facilities at the National University of Loja (Ecuador). Ten second-instar larvae were carefully transferred to the upper leaves of 34-day-old plants using a fine paint brush. Each infested plant was examined for insect damage at 7 dpi (days post-infestation). To this end, plants were harvested one week after infestation (41 days after sowing) by removing the entire plant from the pot. The shoots were cut at the root collar region, the leaves were detached and spread on paper and photographed with a ruler for scaling and assessing insect damage. Leaf damage by *P. longifila* larvae was quantified with ImageJ (Schindelin et al., 2015). This software associates the number of pixels in the pictures with the real scale or ruler to measure the area (mm scale was used). The total leaf area and leaf damage percentages were determined for each plant. The leaf damage percentages were subjected to analysis of variance (ANOVA) with a linear model using the function *lm* in RStudio environment (R 4.3.1) (R Core Team, 2023). The packages dplyr (Wickham et al., 2023) and ggplot2 (Wickham, 2016) were used for data structuring and plotting.

DNA extraction from the tomato rhizosphere for microbiome profiling

Following the harvest of the 41-day-old tomato plants, roots were shaken vigorously to remove loosely attached soil. The root system was then placed into a 15 ml-tube with 4 ml of LifeGuard® Soil Preservation Solution and stored at 4 °C. In the Laboratory of Biotechnology, National University of Loja, the rhizosphere samples were split into three subsamples with 1 g of soil and 1 ml of LifeGuard® Soil Preservation Solution and placed into a 2 ml-microtube and stored at -20 °C until DNA extraction. To extract rhizosphere DNA, the 2-ml microtubes were centrifuged at 10,000 × *g* for 1 min, and the supernatant of LifeGuard® Soil Preservation Solution was discarded. The Qiagen DNeasy® PowerSoil® Kit (Qiagen, USA) was used to isolate the genomic DNA of the remaining soil pellet according to the manufacture's kit protocol. DNA samples were sent to Genome Québec (Canada) for amplicon library preparation and subsequent sequencing of the V3-V4 regions of the 16S rRNA gene using the universal bacterial primers 341F (CCTACGGGNGGCWGCAG) and 805R (GACTACHVGGGTATC-TAATCC). Paired-end sequence reads (300 bp length) were generated using the Illumina NovaSeqX Plus platform. Additionally, shotgun sequencing was performed on eight pooled rhizosphere samples: DNA of five replicates from each treatment were pooled and 20 µl (concentration 20 ng/µl) aliquots were lyophilized and subjected to library preparation and shotgun sequencing to provide paired-end reads of 150 bp by Illumina NovaSeq 6000.

Amplicon data analysis

The compressed sequence reads contained in FASTQ format files were processed by the DADA2 v1.16.0 pipeline (Callahan et al., 2016) in RStudio environment (RStudio Team, 2020) to obtain the ASV abundance and taxonomy tables. The modeling of error rates associated with the sequencing process was adjusted to appropriately process NovaSeq data using the DADA2 pipeline, as previously suggested by Holland-Moritz (2021). The SILVA 16S ribosomal RNA gene reference database (v138) (Quast et al., 2013) was used for bacterial taxonomy assignment. The statistical analyses were performed in RStudio environment and R software version 4.3.1 (R Core Team, 2023). Packages such as vegan (Oksanen et al., 2020), phyloseq (McMurdie & Holmes, 2013), metagenomeSeq (Paulson et al., 2013) and ggplot2 (Wickham, 2016) were used for alpha diversity (ANOVA, Tukey HSD post hoc test), beta diversity (Bray–Curtis distance, PERMANOVA with 9,999 permutations), and differential abundance analyses, while the tidyverse package (Wickham et al., 2019) was used for formatting and visualization. The abundance data were normalized by CSS (Cumulative Sum Scaling) before further analysis. Principal Coordinates Analysis (PCoA) was done using the *cmdscale* function from the vegan package and the Bray–Curtis distance calculated previously. An UpSet plot to determine the shared ASVs among soils was generated by UpSetR software (Lex et al., 2014). Absolute abundance values of bacteria were used in a regression model to analyze their correlation with leaf insect damage percentages.

Metagenome data analysis

The compressed paired-end FASTQ files were processed using SqueezeMeta v1.5.1 (Tamames & Puente-Sánchez, 2019). Co-assembly was done using Megahit (Li et al., 2015). 16S RNAs were predicted with Barrnap (Seemann, 2014) and taxonomically classified using the RDP classifier (Wang et al., 2007). While tRNA/tmRNA sequences were predicted using ARAGORN (Laslett & Canback, 2004). ORFs were predicted using Prodigal (Hyatt et al., 2010). Similarity searches for GenBank (Clark et al., 2016), EggNOG (Huerta-Cepas et al., 2016), KEGG (Kanehisa & Goto, 2000), were done using Diamond (Buchfink et al., 2015). Read mapping against contigs was performed using Bowtie2 (Langmead & Salzberg, 2012) and binning was done using MaxBin2 (Wu et al., 2016) and Metabat2 (Kang et al., 2019). Results from both binning approaches were combined using DAS Tool to obtain refined bins (Sieber et al., 2018). Relevant information from the metagenomics data (ORF, contig and bin annotations, aggregated taxonomic and functional features) was exported into tables by running the SqueezeMeta utility script *sqm2tables.py* (Tamames & Puente-Sánchez, 2019) to facilitate the metadata handling for further analysis.

Bin completeness and contamination were computed using CheckM (Parks et al., 2015). Based on this, and a quality threshold choosing only bins with completeness

higher than 70% and contamination less than 10%, 69 bins were selected (Supplementary Table S1). High-quality bins of unclassified Micromonosporaceae and classified as *Nocardioides* were selected to submit to RAST server (Rapid Annotation using Subsystems Technology) (Aziz et al., 2008) for functional annotation. Also, the bin files were submitted to antiSMASH software (Antibiotics & Secondary Metabolite Analysis Shell) version 7 (Blin et al., 2023) to annotate BGCs (biosynthetic gene clusters) involved in secondary metabolite production.

Figure 7 clarifies the methodological design followed in this chapter:

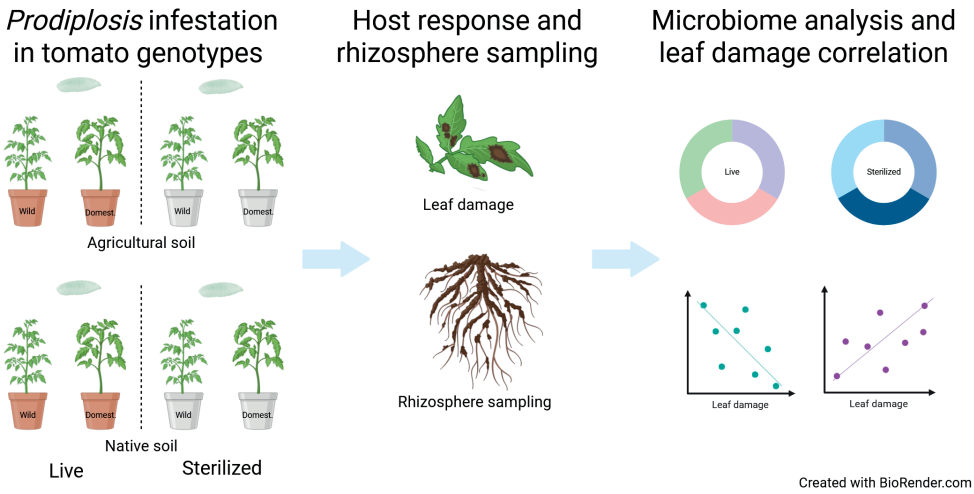

Figure 7. Experimental workflow illustrating the setup of *Prodiplosis longifila* larval infestation in tomato genotypes grown in agricultural and native soils under live or sterilized conditions. Host response was assessed by measuring leaf damage, and rhizosphere samples were collected for microbiome profiling. Microbiome composition was analyzed, and correlations between specific microbiome rhizosphere members and leaf damage were subsequently performed.

Acknowledgements

We would like to express our sincere gratitude to Dr. Max Encalada Córdova, Research Head; Dr. Tulio Solano Castillo, Head of the Phytopathology and Agricultural Microbiology Laboratory; MSc. Jeamel Ruiz Toledo and MSc. Jonny M. Paccha Angamarca, laboratory technicians at Phytopathology and Agricultural Microbiology Laboratory; Dr. Edmigio Valdivieso Caraguay, Head of the Germplasm Bank; Dr. Franklin Román Cárdenas, Head of the Biotechnology Laboratory; and, MSc. Jaime Peña Tamayo, botanist of the Herbarium Loja at the National University of Loja. Their invaluable contributions and assistance throughout the experimental stage —by providing greenhouse and laboratory facilities, insect handling techniques, plant identification of tomato-associated species in the field, as well as wild tomato seeds for the experiment— were essential to achieving our goals. We thank Dr. Sonia Zapata and Juan Mosquera at the Universidad San Francisco de Quito (USFQ) for their support with the research permit procedures, and we thank the USFQ Microbiology Institute for their laboratory facilities and support.

Author contributions

SSF: methodology, investigation, data curation; writing - original draft, review & editing; VC: writing - review & editing; data curation; BOO: investigation, data analysis; writing - review & editing; LMAG: data curation; visualization; review & editing; NS: data curation; JMR: conceptualization; supervision; funding acquisition, writing - review & editing; PVTH: supervision; review & editing. All authors contributed critically to the drafts and gave final approval for publication.

Data availability

Raw 16S and shotgun metagenomics sequences were submitted to the European Nucleotide Archive (ENA) under the project accession number PRJEB82448.

Conflict of interest

No conflict of interest declared

Funding

This research was supported by the Dutch Research Council [Grant/Award number 024.004.014], the Ecuadorian National Secretary of Higher Education, Science, Technology and Innovation–SENESCYT [scholarship number CZ07-000440-2018 to SSF] and, Chancellor Grant and COCIBA–USFQ research funds [HUBI project ID: 10093 entitled "Going back to the roots: Root microbiomes of tomato relatives" to PVH]. The funders had no role in the study design, data collection, analysis, decision to publish, or preparation of the manuscript.

Plant research permit

This study was carried out under the Genetic Resource Permit N° MAE-DNB-CM-2018-0085, issued by the Ministry of Environment of Ecuador to USFQ.

Supplementary material

Supplementary Figures

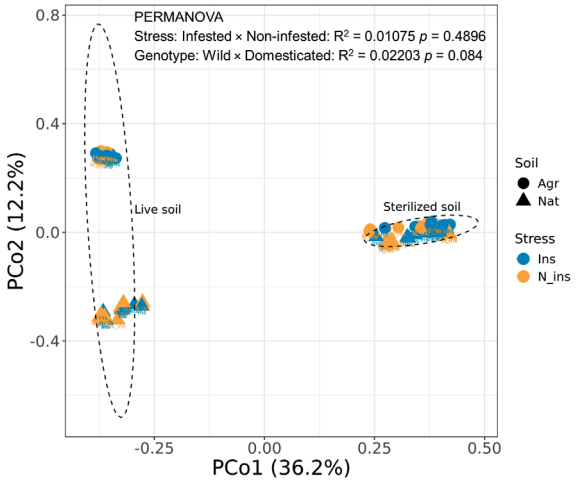

Figure S1. PCoA of bacterial communities in the rhizosphere of domesticated *S. lycopersicum* cv. Moneymaker and wild *S. pimpinellifolium* tomato. The analysis constrasts infested (Ins) and non-infested (N_ins) plants by *Prodiplosis longifila* considering different soil types (Agr: agricultural vs. Nat: native) and soil conditions (Live vs. Sterilized).

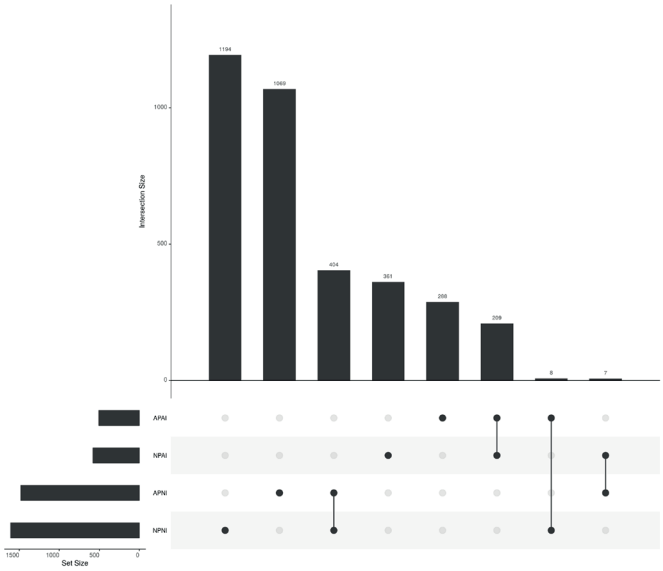

Figure S2. Number of bacterial ASVs shared among wild tomato *S. pimpinellifolium* rhizosphere samples. APAI: sterilized agricultural soil; NPAI: sterilized native soil; APNI: live agricultural soil; NPNI: live native soil. Upset plot generated by UpSetR software https://gehlenborglab.shinyapps.io/upsetr/ (Lex et al., 2014).

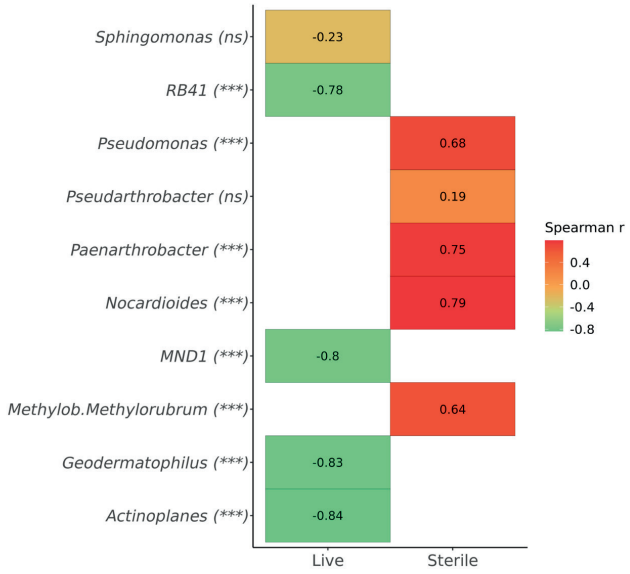

Figure S3. Heatmap of Spearman correlation coefficients between highest abundant rhizosphere bacteria genera in live and sterile soil and leaf damage proportion of *Solanum pimpinellifolium* infested by *Prodiplosis longifila.* Significance of the correlation is shown in parenthesis ($p < 0.05$ *, $p < 0.01$ **, $p < 0.001$ ***, ns: not significant).

Overview | 2.1 | 14.1 | 32.1 | 53.1 | 118.1 | 141.1 | 155.1 | 205.1 | 262.1 | 271.1 | 276.1

Identified secondary metabolite regions using strictness 'relaxed'

Region	Type	From	To	Most similar known cluster		Similarity
Region 2.1	T3PKS	18,038	41,232	loseolamycin A1/loseolamycin A2	Polyketide	64%
Region 14.1	lanthipeptide-class-i	1	8,932			
Region 32.1	NAPAA	1	23,977	stenothricin	NRP:Cyclic depsipeptide	13%
Region 53.1	RiPP-like	1	7,880			
Region 118.1	crocagin	1	18,092			
Region 141.1	aminopolycarboxylic-acid	42,937	56,354	EDHA	Other	88%
Region 155.1	terpene	1	10,650	isorenieratene	Terpene	25%
Region 205.1	PKS-like	1	27,176			
Region 262.1	lanthipeptide-class-iii	1	13,836			
Region 271.1	T3PKS	1	11,455	glycinocin A	NRP	4%
Region 276.1	NI-siderophore	10,146	23,156			

Figure S4. Overview of BGCs found in Micromonosporaceae bin 580 (*Actinoplanes* family) by bacterial antiSMASH software (Blin et al., 2023).

Overview | 252.1

Identified secondary metabolite regions using strictness 'relaxed'

Region	Type	From	To	Most similar known cluster	Similarity
Region 252.1	RRE-containing	1	2,627		

Figure S5. Overview of BGCs found in *Nocardioides* bin 2.78 by bacterial antiSMASH software (Blin et al., 2023).

Table S1. High quality-bins assembled by SqueezeMeta from rhizosphere tomato soil infested by *Prodiplosis longifila*.

Bin_ID	Marker_lineage	Completeness	Contamination	Method	Kingdom	Phylum	Class	Order	Family	Genus	Species	Length	GC_perc	Num_contigs	Sum_TPM_live	Sum_TPM_sterile
maxbin.003.fasta.contigs	p__Bacteroidetes (UID2591)	96.55	4.06	DAS	Bacteria	Bacteroidetes	Chitinophagia	Chitinophagales	Chitinophagaceae	NA	NA	4,923,528	43.67	129	457.062	4150.131
maxbin.004.fasta.contigs	f__Burkholderiaceae (UID4003)	90.15	4.55	DAS	Bacteria	Proteobacteria	Betaproteobacteria	Burkholderiales	Burkholderiaceae	Ralstonia	NA	5,392,280	63.79	231	330.483	426.983
maxbin.006.fasta.contigs	k__Bacteria (UID2565)	80.83	2.55	DAS	Bacteria	Planctomycetes	NA	NA	NA	NA	NA	7,911,020	57.54	209	252.583	25727.007
maxbin.009.fasta.contigs	c__Alphaproteobacteria (UID3422)	75.98	9.96	DAS	Bacteria	Proteobacteria	Alphaproteobacteria	Caulobacterales	Caulobacteraceae	Phenylobacterium	NA	4,588,661	69.98	510	1140.756	11075.45
maxbin.012.fasta.contigs	k__Bacteria (UID2495)	76.86	2	DAS	Bacteria	Gemmatimonadetes	Gemmatimonadetes	Gemmatimonadales	Gemmatimonadaceae	NA	NA	3,142,557	63.65	58	280.254	2585.52
maxbin.016.fasta.contigs	c__Gammaproteobacteria (UID4444)	91.66	9.05	DAS	Bacteria	Proteobacteria	Gammaproteobacteria	NA	NA	NA	NA	4,526,198	43.53	773	147.539	9452.228
maxbin.044.fasta.contigs	k__Bacteria (UID2982)	81.01	3.9	DAS	Bacteria	Verrucomicrobia	NA	NA	NA	NA	NA	6,768,386	60.92	1067	778.821	6882.065
maxbin.049.fasta.contigs	k__Bacteria (UID2982)	79.64	8.97	DAS	Bacteria	Verrucomicrobia	NA	NA	NA	NA	NA	5,301,187	51.66	245	259.691	5832.157
maxbin.097.fasta.contigs	c__Betaproteobacteria (UID3959)	94.15	5.89	DAS	Bacteria	Proteobacteria	Betaproteobacteria	Burkholderiales	NA	NA	NA	3,767,025	60.82	188	579.976	5384.284
maxbin.104.fasta.contigs	c__Alphaproteobacteria (UID3305)	83.62	4.59	DAS	Bacteria	Proteobacteria	Alphaproteobacteria	NA	NA	NA	NA	3,677,311	62.55	134	784.742	4135.142
maxbin.145.fasta.contigs	p__Bacteroidetes (UID2591)	84.89	5.57	DAS	Bacteria	Bacteroidetes	Chitinophagia	Chitinophagales	NA	NA	NA	3,707,379	43.52	1076	220.066	6235.133

Table S1. High quality-bins assembled by SqueezeMeta from rhizosphere tomato soil infested by *Prodiplosis longifila*. (*continued*)

Bin_ID	Marker_lineage	Completeness	Contamination	Method	Kingdom	Phylum	Class	Order	Family	Genus	Species	Length	GC_perc	Num_contigs	Sum_TPM_live	Sum_TPM_sterile
maxbin.188.fasta.contigs	f__Halobacteriaceae (UID85)	94.73	2.93	DAS	Archaea	Euryarchaeota	Halobacteria	Natrialbales	Natrialbaceae	NA	NA	4,061,149	66.71	360	3775.17	3205.368
maxbin.218.fasta.contigs	k__Bacteria (UID2982)	81.64	7.98	DAS	Bacteria	Verrucomicrobia	NA	NA	NA	NA	NA	5,483,094	51.65	603	434.351	11558.335
maxbin.247.fasta.contigs	k__Bacteria (UID2570)	91.8	2.73	DAS	Bacteria	NA	NA	NA	NA	NA	NA	5,275,354	61.75	544	278.328	7867.893
maxbin.360.fasta.contigs	k__Bacteria (UID203)	76.03	0	DAS	Bacteria	Proteobacteria	Gammaproteobacteria	Xanthomonadales	NA	NA	NA	2,285,668	70.25	115	1561.343	7483.135
maxbin.371.fasta.contigs	p__Bacteroidetes (UID2591)	99.01	0.25	DAS	Bacteria	Bacteroidetes	Chitinophagia	Chitinophagales	Chitinophagaceae	Chitinophaga	Chitinophaga sancti	5,853,332	42.46	132	272.215	7062.444
maxbin.414.fasta.contigs	o__Burkholderiales (UID4002)	89.92	9.74	DAS	Bacteria	Proteobacteria	Betaproteobacteria	Burkholderiales	Oxalobacteraceae	NA	NA	6,142,809	62.63	460	4255.204	906.804
maxbin.415.fasta.contigs	p__Bacteroidetes (UID2605)	95	3.65	DAS	Bacteria	Bacteroidetes	NA	NA	NA	NA	NA	4,687,430	45.72	663	235.57	5912.872
maxbin.432.fasta_sub.contigs	k__Bacteria (UID203)	83.54	8.23	DAS	Bacteria	Proteobacteria	Gammaproteobacteria	Xanthomonadales	NA	NA	NA	2,798,466	64.76	197	342.66	198.749
maxbin.464.fasta.contigs	p__Bacteroidetes (UID2591)	92.86	4.2	DAS	Bacteria	Bacteroidetes	Chitinophagia	Chitinophagales	Chitinophagaceae	NA	NA	7,536,217	47.12	386	1033.659	6339.271
maxbin.468.fasta.contigs	p__Bacteroidetes (UID2591)	95.76	5.62	DAS	Bacteria	Bacteroidetes	Chitinophagia	Chitinophagales	Chitinophagaceae	NA	NA	4,932,603	40.25	609	434.125	5474.293
maxbin.472.fasta_sub.contigs	f__Micrococcaceae (UID1631)	87.84	4.74	DAS	Bacteria	Actinobacteria	Actinomycetia	Micrococcales	Micrococcaceae	NA	NA	3,806,130	66.71	943	5044.113	11672.052

Table S1. High quality-bins assembled by SqueezeMeta from rhizosphere tomato soil infested by *Prodiplosis longifila*. (*continued*)

Bin_ID	Marker_lineage	Completeness	Contamination	Method	Kingdom	Phylum	Class	Order	Family	Genus	Species	Length	GC_perc	Num_contigs	Sum_TPM_live	Sum_TPM_sterile
maxbin.476.fasta_sub.contigs	k__Bacteria (UID2982)	78.41	8.11	DAS	Bacteria	Verrucomicrobia	NA	NA	NA	NA	NA	6,669,823	61.47	1084	503.843	4178.324
maxbin.489.fasta.contigs	k__Bacteria (UID203)	100	9.69	DAS		NA	NA	NA	NA	NA	NA	7,097,239	36.7	331	133.742	10946.075
maxbin.508.fasta.contigs	c__Alphaproteobacteria (UID3305)	76.73	6.79	DAS	Bacteria	Proteobacteria	Alphaproteobacteria	Sphingomonadales	Sphingomonadaceae	Sphingomonas	NA	2,056,600	64.38	622	20498.528	450.123
maxbin.515.fasta.contigs	k__Bacteria (UID203)	75.71	7.55	DAS	Bacteria	NA	NA	NA	NA	NA	NA	1,664,664	47.24	268	241.725	4556.406
maxbin.527.fasta.contigs	k__Bacteria (UID2982)	86.54	3.38	DAS	Bacteria	NA	NA	NA	NA	NA	NA	1,830,959	43.94	213	73,452	3544,979
maxbin.531.fasta.contigs	k__Bacteria (UID2495)	92.28	2.37	DAS	Bacteria	Spirochaetes	Spirochaetia	Leptospirales	Leptospiraceae	Leptospira	NA	3,935,131	40.24	1188	152,639	3064,683
maxbin.568.fasta.contigs	o__Cytophagales (UID2936)	93.71	3.63	DAS	Bacteria	Bacteroidetes	NA	NA	NA	NA	NA	5,298,703	45.68	456	683,266	4101,769
maxbin.580.fasta.contigs	o__Actinomycetales (UID1696)	88.42	2.59	DAS	Bacteria	Actinobacteria	Actinomycetia	Micromonosporales	Micromonosporaceae	NA	NA	4,880,819	70.03	320	67231,883	263,036
maxbin.587.fasta.contigs	k__Bacteria (UID2982)	88.4	7.25	DAS	Bacteria	Verrucomicrobia	NA	NA	NA	NA	NA	5,712,602	52.19	1052	393,692	184,614
maxbin.605.fasta.contigs	f__Enterobacteriaceae (UID5124)	96.22	2.01	DAS	Bacteria	Proteobacteria	Gammaproteobacteria	Enterobacterales	Enterobacteriaceae	NA	NA	4,609,621	56.05	334	91,803	4388,719
maxbin.658.fasta.contigs	k__Bacteria (UID2495)	93.13	7.89	DAS	Bacteria	Gemmatimonadetes	NA	NA	NA	NA	NA	3,353,775	59.82	462	12963,416	14,967
maxbin.673.fasta.contigs	p__Cyanobacteria (UID2189)	95.54	9.63	DAS	Bacteria	Cyanobacteria	NA	NA	NA	NA	NA	9,710,549	46.33	1710	2511,263	4,375
maxbin.683.fasta.contigs	k__Archaea (UID2)	90.78	3.88	DAS	Archaea	Thaumarchaeota	NA	NA	NA	NA	NA	1,783,922	50.62	413	30006,247	13,96

Table S1. High quality-bins assembled by SqueezeMeta from rhizosphere tomato soil infested by *Prodiplosis longifila*. (*continued*)

Bin_ID	Marker_lineage	Completeness	Contamination	Method	Kingdom	Phylum	Class	Order	Family	Genus	Species	Length	GC_perc	Num_contigs	Sum_TPM_live	Sum_TPM_sterile
metabat2.1.fa.contigs	o__Sphingomonadales (UID3310)	70.52	0.69	DAS	Bacteria	Proteobacteria	Alphaproteobacteria	Sphingomonadales	Sphingomonadaceae	NA	NA	2,289,747	67.64	129	372,298	5678,63
metabat2.135.fa.contigs	o__Burkholderiales (UID4002)	71.97	1.91	DAS	Bacteria	Proteobacteria	Betaproteobacteria	Burkholderiales	Oxalobacteraceae	NA	NA	4,368,555	59.27	608	6516,666	145,848
metabat2.136.fa_sub.contigs	o__Cytophagales (UID2936)	83.05	1.04	DAS	Bacteria	Bacteroidetes	Cytophagia	Cytophagales	NA	NA	NA	5,256,850	48.07	277	787,309	1005,646
metabat2.157.fa.contigs	k__Bacteria (UID203)	78.09	5.17	DAS	Bacteria	Verrucomicrobia	Verrucomicrobiae	Verrucomicrobiales	Verrucomicrobiaceae	NA	NA	4,236,708	60.27	496	281,688	214,139
metabat2.158.fa_sub.contigs	k__Bacteria (UID3187)	81.42	8.55	DAS	Bacteria	Acidobacteria	NA	NA	NA	NA	NA	3,907,414	66.84	543	1878,565	2023,782
metabat2.159.fa.contigs	o__Cytophagales (UID2936)	85.85	1.49	DAS	Bacteria	Bacteroidetes	Cytophagia	Cytophagales	NA	NA	NA	5,162,706	46.72	542	781,227	129,77
metabat2.18.fa.contigs	p__Cyanobacteria (UID2182)	96.7	1.18	DAS	Bacteria	Cyanobacteria	NA	NA	NA	NA	NA	5,852,500	47.66	304	8101,354	4,371
metabat2.190.fa.contigs	p__Bacteroidetes (UID2591)	75.52	2.22	DAS	Bacteria	Bacteroidetes	Chitinophagia	Chitinophagales	Chitinophagaceae	NA	NA	3,332,901	56.47	461	366,619	4627,984
metabat2.204.fa.contigs	k__Bacteria (UID2495)	70.16	4.4	DAS	Bacteria	Gemmatimonadetes	NA	NA	NA	NA	NA	2,822,695	64	414	491,866	1060,357
metabat2.206.fa_sub.contigs	k__Bacteria (UID1453)	80.57	2.85	DAS	Bacteria	Actinobacteria	NA	NA	NA	NA	NA	3,174,811	69.85	234	794,576	2570,79
metabat2.21.fa.contigs	o__Bacillales (UID828)	87.43	2.54	DAS	Bacteria	Firmicutes	Bacilli	Bacillales	Bacillaceae	Priestia	NA	3,754,103	38.34	598	1972,028	2861,669
metabat2.232.fa_sub.contigs	f__Burkholderiaceae (UID4003)	92.79	2.87	DAS	Bacteria	Proteobacteria	Betaproteobacteria	Burkholderiales	Burkholderiaceae	Cupriavidus	NA	5,740,917	66.3	428	480,622	5670,952

Table S1. High quality-bins assembled by SqueezeMeta from rhizosphere tomato soil infested by *Prodiplosis longifila*. (*continued*)

Bin_ID	Marker_lineage	Completeness	Contamination	Method	Kingdom	Phylum	Class	Order	Family	Genus	Species	Length	GC_perc	Num_contigs	Sum_TPM_live	Sum_TPM_sterile
metabat2.239.fa.contigs	c__Alphaproteobacteria (UID3422)	81.08	3.01	DAS	Bacteria	Proteobacteria	Alphaproteobacteria	NA	NA	NA	NA	2,983,850	62.33	436	514,32	1186,826
metabat2.24.fa.contigs	k__Bacteria (UID1453)	74.03	3.78	DAS	Bacteria	Actinobacteria	Acidimicrobiia	NA	NA	NA	NA	2,901,287	71.54	398	1179,018	2732,154
metabat2.262.fa.contigs	k__Bacteria (UID203)	78.45	0.86	DAS	Bacteria	Proteobacteria	Betaproteobacteria	Burkholderiales	NA	NA	NA	3,011,244	70.62	284	9017,283	4584,655
metabat2.273.fa.contigs	c__Alphaproteobacteria (UID3305)	85.94	1.52	DAS	Bacteria	Proteobacteria	Alphaproteobacteria	Sphingomonadales	NA	NA	NA	2,716,380	59.39	90	101,235	2276,446
metabat2.274.fa_sub.contigs	p__Bacteroidetes (UID2591)	97.37	0.74	DAS	Bacteria	Bacteroidetes	Chitinophagia	Chitinophagales	Chitinophagaceae	Chitinophaga	Chitinophaga sancti	6,896,030	45.02	233	83,436	9557,47
metabat2.277.fa_sub.contigs	c__Alphaproteobacteria (UID3305)	78.98	5.71	DAS	Bacteria	Proteobacteria	Alphaproteobacteria	Sphingomonadales	Sphingomonadaceae	Sphingomonas	NA	2,037,372	67.47	351	925,647	925,536
metabat2.288.fa.contigs	k__Archaea (UID2)	79.13	5.34	DAS	Archaea	Thaumarchaeota	NA	NA	NA	NA	NA	1,403,343	35.85	186	8392,975	4,695
metabat2.304.fa.contigs	c__Alphaproteobacteria (UID3305)	76.63	4.5	DAS	Bacteria	Proteobacteria	Alphaproteobacteria	Sphingomonadales	Sphingomonadaceae	Sphingomonas	NA	1,763,881	64.57	238	1393,536	3031,039
metabat2.305.fa.contigs	p__Cyanobacteria (UID2189)	86.44	2.01	DAS	Bacteria	Cyanobacteria	NA	NA	NA	NA	NA	7,075,742	46.75	349	14366,768	2,988
metabat2.353.fa_sub.contigs	f__Micrococcaceae (UID1631)	95.18	1.16	DAS	Bacteria	Actinobacteria	Actinomycetia	Micrococcales	Micrococcaceae	NA	NA	4,100,067	63.68	122	361,341	9011,369
metabat2.358.fa.contigs	c__Betaproteobacteria (UID3959)	74.92	3.4	DAS	Bacteria	Proteobacteria	Betaproteobacteria	Burkholderiales	Alcaligenaceae	Bordetella	Bordetella bronchialis	4,349,268	67.69	821	441,811	3314,553

Table S1. High quality-bins assembled by SqueezeMeta from rhizosphere tomato soil infested by *Prodiplosis longifila*. (*continued*)

Bin_ID	Marker_lineage	Completeness	Contamination	Method	Kingdom	Phylum	Class	Order	Family	Genus	Species	Length	GC_perc	Num_contigs	Sum_TPM_live	Sum_TPM_sterile
metabat2.37.fa.contigs	c__Betaproteobacteria (UID3959)	72.73	1.24	DAS	Bacteria	Proteobacteria	Betaproteobacteria	NA	NA	NA	NA	3,062,315	61.47	175	535,807	2006,992
metabat2.38.fa.contigs	c__Betaproteobacteria (UID3959)	75.22	1.31	DAS	Bacteria	Proteobacteria	Betaproteobacteria	NA	NA	NA	NA	3,865,322	58.63	592	354,853	2908,733
metabat2.384.fa.contigs	o__Burkholderiales (UID4000)	83.95	1.79	DAS	Bacteria	Proteobacteria	Betaproteobacteria	Burkholderiales	Comamonadaceae	Variovorax	NA	4,889,619	70.84	462	1449,913	11890,59
metabat2.390.fa.contigs	c__Deltaproteobacteria (UID3216)	74.87	3.46	DAS	Bacteria	Proteobacteria	Deltaproteobacteria	Myxococcales	NA	NA	NA	6,426,917	65.86	349	1506,687	4559,171
metabat2.45.fa_sub.contigs	k__Bacteria (UID203)	74.29	3.45	DAS	Bacteria	Bacteroidetes	NA	NA	NA	NA	NA	3,021,302	36.75	349	3908,152	1225,417
metabat2.48.fa_sub.contigs	p__Bacteroidetes (UID2591)	81.4	1.97	DAS	Bacteria	Bacteroidetes	Chitinophagia	Chitinophagales	Chitinophagaceae	Niastella	NA	6,436,456	44.26	476	1161,871	6493,219
metabat2.59.fa_sub.contigs	o__Burkholderiales (UID4000)	78.63	3.68	DAS	Bacteria	Proteobacteria	Betaproteobacteria	Burkholderiales	Comamonadaceae	Variovorax	NA	4,352,969	68.35	638	1021,628	4187,495
metabat2.70.fa.contigs	o__Burkholderiales (UID4000)	84.41	3.13	DAS	Bacteria	Proteobacteria	Betaproteobacteria	Burkholderiales	NA	NA	NA	3,699,209	69.39	417	1871,94	3296,182
metabat2.78.fa_sub.contigs	o__Actinomycetales (UID1697)	72.6	5.66	DAS	Bacteria	Actinobacteria	Actinomycetia	Propionibacteriales	Nocardioidaceae	Nocardioides	NA	3,223,870	72.41	385	1566,67	9182,806
metabat2.95.fa.contigs	k__Bacteria (UID2982)	77.45	2.49	DAS	Bacteria	Verrucomicrobia	Verrucomicrobiae	Verrucomicrobiales	NA	NA	NA	4,526,054	61.25	692	319,887	3374,055
metabat2.97.fa.contigs	o__Burkholderiales (UID4000)	75.29	2.6	DAS	Bacteria	Proteobacteria	Betaproteobacteria	Burkholderiales	Comamonadaceae	NA	NA	2,332,583	69.16	339	3957,81	3068,633

Table S2. Annotated protein encoding genes by RAST server using the SEED Subsystem database from bacterial assembled bins of tomato rhizosphere

bin_name	Category	Subcategory	Subsystem	Role	Features
Micromonosporaceae_bin580	Phages, Prophages, Transposable elements, Plasmids	Phages, Prophages	Phage packaging machinery	Phage terminase, large subunit	fig|6666666.1083232.peg.2626, fig|6666666.1083232.peg.4401
Micromonosporaceae_bin580	Phages, Prophages, Transposable elements, Plasmids	Phages, Prophages	Phage lysis modules	Phage holin	fig|6666666.1083232.peg.1045
Micromonosporaceae_bin580	Phages, Prophages, Transposable elements, Plasmids	Phages, Prophages	Phage lysis modules	Phage endolysin	fig|6666666.1083232.peg.653, fig|6666666.1083232.peg.3139
Micromonosporaceae_bin580	Phages, Prophages, Transposable elements, Plasmids	Phages, Prophages	Phage lysis modules	Phage lysin, 1,4-beta-N-acetylmuramidase (EC 3.2.1.17) or lysozyme	fig|6666666.1083232.peg.243
Micromonosporaceae_bin580	Iron acquisition and metabolism	Iron acquisition and metabolism - no subcategory	Ferrous iron transporter EfeUOB, low-pH-induced	Ferrous iron transport peroxidase EfeB	fig|6666666.1083232.peg.3765
Micromonosporaceae_bin580	Iron acquisition and metabolism	Iron acquisition and metabolism - no subcategory	Ferrous iron transporter EfeUOB, low-pH-induced	Ferrous iron transport periplasmic protein EfeO, contains peptidase-M75 domain and (frequently) cupredoxin-like domain	fig|6666666.1083232.peg.3766
Micromonosporaceae_bin580	Iron acquisition and metabolism	Iron acquisition and metabolism - no subcategory	Ferrous iron transporter EfeUOB, low-pH-induced	Ferrous iron transport permease EfeU	fig|6666666.1083232.peg.3767
Micromonosporaceae_bin580	Dormancy and Sporulation	Dormancy and Sporulation - no subcategory	Sporulation-associated proteins with broader functions	Peptidyl-tRNA hydrolase (EC 3.1.1.29)	fig|6666666.1083232.peg.1609
Micromonosporaceae_bin580	Respiration	Electron donating reactions	Respiratory dehydrogenases 1	NADH dehydrogenase (EC 1.6.99.3)	fig|6666666.1083232.peg.1191, fig|6666666.1083232.peg.2346, fig|6666666.1083232.peg.2614, fig|6666666.1083232.peg.4063

Table S2. Annotated protein encoding genes by RAST server using the SEED Subsystem database from bacterial assembled bins of tomato rhizosphere (*continued*)

bin_name	Category	Subcategory	Subsystem	Role	Features
Micromonosporaceae_bin580	Respiration	Electron donating reactions	Respiratory Complex I	NADH-ubiquinone oxidoreductase chain E (EC 1.6.5.3)	fig|6666666.1083232.peg.4653
Micromonosporaceae_bin580	Respiration	Electron donating reactions	Respiratory Complex I	NADH ubiquinone oxidoreductase chain A (EC 1.6.5.3)	fig|6666666.1083232.peg.1691, fig|6666666.1083232.peg.3401, fig|6666666.1083232.peg.4657
Micromonosporaceae_bin580	Respiration	Electron donating reactions	Respiratory Complex I	NADH-ubiquinone oxidoreductase chain C (EC 1.6.5.3)	fig|6666666.1083232.peg.3158, fig|6666666.1083232.peg.3398, fig|6666666.1083232.peg.4655
Micromonosporaceae_bin580	Respiration	Electron donating reactions	Respiratory Complex I	NADH-ubiquinone oxidoreductase chain H (EC 1.6.5.3)	fig|6666666.1083232.peg.3397, fig|6666666.1083232.peg.4650
Micromonosporaceae_bin580	Respiration	Electron donating reactions	Respiratory Complex I	NADH-ubiquinone oxidoreductase chain J (EC 1.6.5.3)	fig|6666666.1083232.peg.4648
Micromonosporaceae_bin580	Respiration	Electron donating reactions	Respiratory Complex I	NADH-ubiquinone oxidoreductase chain F (EC 1.6.5.3)	fig|6666666.1083232.peg.4652
Micromonosporaceae_bin580	Respiration	Electron donating reactions	Respiratory Complex I	NADH-ubiquinone oxidoreductase chain N (EC 1.6.5.3)	fig|6666666.1083232.peg.3391, fig|6666666.1083232.peg.4644
Micromonosporaceae_bin580	Respiration	Electron donating reactions	Respiratory Complex I	NADH-ubiquinone oxidoreductase chain M (EC 1.6.5.3)	fig|6666666.1083232.peg.3392, fig|6666666.1083232.peg.4645
Micromonosporaceae_bin580	Respiration	Electron donating reactions	Respiratory Complex I	NADH-ubiquinone oxidoreductase chain K (EC 1.6.5.3)	fig|6666666.1083232.peg.3394, fig|6666666.1083232.peg.4647

Table S2. Annotated protein encoding genes by RAST server using the SEED Subsystem database from bacterial assembled bins of tomato rhizosphere (*continued*)

bin_name	Category	Subcategory	Subsystem	Role	Features
Micromonosporaceae_bin580	Respiration	Electron donating reactions	Respiratory Complex I	NADH-ubiquinone oxidoreductase chain B (EC 1.6.5.3)	fig|6666666.1083232.peg.3157, fig|6666666.1083232.peg.3400, fig|6666666.1083232.peg.4656
Micromonosporaceae_bin580	Respiration	Electron donating reactions	Respiratory Complex I	NADH-ubiquinone oxidoreductase chain I (EC 1.6.5.3)	fig|6666666.1083232.peg.3396, fig|6666666.1083232.peg.4649
Micromonosporaceae_bin580	Respiration	Electron donating reactions	Respiratory Complex I	NAD(P)H-quinone oxidoreductase chain J (EC 1.6.5.2)	fig|6666666.1083232.peg.3395
Micromonosporaceae_bin580	Respiration	Electron donating reactions	Respiratory Complex I	NADH-ubiquinone oxidoreductase chain L (EC 1.6.5.3)	fig|6666666.1083232.peg.3393, fig|6666666.1083232.peg.4646
Micromonosporaceae_bin580	Respiration	Electron donating reactions	Respiratory Complex I	NADH-ubiquinone oxidoreductase chain D (EC 1.6.5.3)	fig|6666666.1083232.peg.2571, fig|6666666.1083232.peg.3159, fig|6666666.1083232.peg.4654
Micromonosporaceae_bin580	Respiration	Electron donating reactions	Respiratory Complex I	NADH-ubiquinone oxidoreductase chain G (EC 1.6.5.3)	fig|6666666.1083232.peg.4651
Micromonosporaceae_bin580	Respiration	Electron donating reactions	NADH ubiquinone oxidoreductase	NADH-ubiquinone oxidoreductase chain M (EC 1.6.5.3)	fig|6666666.1083232.peg.3392, fig|6666666.1083232.peg.4645
Micromonosporaceae_bin580	Phages, Prophages, Transposable elements, Plasmids	Phages, Prophages	Phage packaging machinery	Phage terminase, large subunit	fig|6666666.1083232.peg.2626, fig|6666666.1083232.peg.4401

Note. The full Table S2 is available online at https://doi.org/10.5281/zenodo.15725118